

Explosion risks at small LNG sites

Graham Atkinson[1], Edmund Cowpe[2], David Painter[2] and Jacqueline Patel[1]
[1] Health and Safety Laboratory, Harpur Hill, Buxton SK17 9JN.
2 Health and Safety Executive, Redgrave Court, Merton Road, Bootle L20 7HS

There have been a number of cases of vapour cloud explosions in which flame acceleration appears to have been driven by the congestion and confinement provided by closely spaced tankers or other heavy goods vehicles. An example of such an incident is the Vapour Cloud Explosion VCE that occurred at Saint Herblain near Nantes in October 1991 (Lechaudel and Mouilleau 1995). Over a period of around 20 minutes, in very low wind speed conditions, a spray release of gasoline formed a low lying cloud. The VCE that followed was powerful enough to crush and overturn tankers as well as breaking windows up to 1000m from the site. An increase in crush and displacement effects along a line of tankers is apparent in photographs of the aftermath. This is consistent with flame acceleration along the line of congested and semi-confined volumes under the vehicles. No other areas with significant potential for flame acceleration were noted by investigators. Computational Fluid Dynamics (CFD) analyses using the AUTOREAGAS code supported the suggestion that flame acceleration occurred under the tankers.

A similar problem may arise with other types of heavy goods vehicle (HGV) if these are parked closely together in areas that may be affected by a low lying vapour cloud. One example of such a situation is a distribution centre served by a fleet of liquid natural gas (LNG) powered HGVs (Figure 1). Such sites may require a substantial inventory of (LNG) to refuel vehicles. In the event of a loss of containment in relatively calm conditions the space under parked trailers (with or without their tractor units) may become flooded with LNG vapour. If the wind speed is close to zero, the vapour cloud may be highly homogenous and potentially, depending on the details of entrainment near the source, close to the stoichiometric ratio.

Experimental work on linear arrays

The majority of experimental work done on flame acceleration in arrays of obstacles has been carried out in enclosed ducts or tubes or in a spherical geometry. Empirical correlations for flame speed have been derived from this work: for example the GAMES methodology (based on experiments with spherically spreading flames) relates the explosion pressure to the laminar flame speed of the mixture, the volume blockage ratio, size of obstacles and the distance from the centre which the flame spreads (Mercx et al 1998). Flame speed and explosion pressure increase rapidly and without limit with the distance over which the flame propagates. Direct application of this type of model to the problem of flame propagation in very long linear arrays tends to predict very severe explosion pressures in all circumstances.

Experiments in open, linear arrays suggest, however, that this unlimited flame acceleration does not always occur in such arrays. Three data sets are of particular value:

1. **British Gas experiments** (Harris and Wickens 1989) These involved methane and other gases in a 45 m long rig. Grids of pipes (normally with a blockage ratio of 40%) at regular intervals drove flame acceleration. The cross section of the linear arrays was 3 x 3 m.

2. **Baker Risk experiments** (Pierorazio et al 2005) These tests involved methane and other gases in a rig where flames could spread for about 7 m. Flame acceleration was driven by vertical 2" diameter pipes in a relatively uniform array. The cross section of the linear arrays was approximately 1.8 x 3.6 m

3. **Buncefield Phase II JIP** (SCI 2014). These tests involved near stoichiometric propane in a rig where flame could spread up to 100m. Flame acceleration was driven by arrays of tree branches. The cross section of the linear arrays was varied between 1 x 3 m and 4.5 x 3 m.

In all of these experimental sets it was observed that flames in open, linear arrays can show an initial phase of rapid acceleration and then propagate steadily – at subsonic speeds. The maximum explosion pressure is then independent of the length of the array. In the Buncefield Phase II JIP steady flame speeds in the range 65- 145 m/s were observed – depending on the type of obstacle array. Narrow arrays (where the array width was comparable to the flame thickness) showed lower flame speeds. Wide arrays or those with more densely packed branches showed higher flame speeds. In the British Gas experiments on stoichiometric methane the flame speed rose to around 80 m/s and then remained constant along the rest of the rig.

In all of the experiments it was observed that for the most reactive gases and most closely packed obstacles the flame speed might "run away". In these cases the speed increased rapidly without limit until deflagration to detonation transition (DDT) occurred. In experiments on propane or other higher hydrocarbons with flame paths longer than about 15m where the flame had a chance to achieve a steady state or run way (i.e British Gas and Buncefield Phase II tests) the outcome was either a relatively low flame speed (<150 m/s) or an unlimited increase in flame speed and DDT. No steady flames with speeds greater than 150 m/s were observed. Some intermediate flame speeds were reported by Baker Risk but the restricted flame path means that these flames were probably accelerating as they reached the end of the rig. The maximum flame speed in the Baker risk experiments was inferred from pressure measurements rather than being measured directly.

Modelling of flame propagation in linear arrays

The modelling of high speed premixed combustion of the higher hydrocarbons from first principles is not possible even with the most advanced CFD. Some commercial codes are available that implement approximate solutions. Typically these represent the relationship between turbulence and acceleration in burning using a simplified expression such as that due to Bray (1990).

$$\frac{S_T}{S_L} = 0.875 Ka^{0.392} \frac{u'}{S_L} \qquad \text{where} \quad Ka = 0.157 \left(\frac{u'}{S_L} \right)^2 \mathrm{Re}'^{-\frac{1}{2}} \quad \text{and} \quad \mathrm{Re}' = \frac{u'.D}{\upsilon}$$

There is also generally an empirically based enhancement factor that accounts for the increase in burning area caused by folding of the flame around obstacles. The codes rely heavily on phenomenological sub-models and have been tuned to match data sets. As noted previously there are very few data available for open linear explosions so the models have typically been tuned by comparison with test explosions in tubes or other enclosed spaces or in spherical geometries (e.g. MERGE). These tests and model solutions typically involve continuously accelerating flames.

Recent work by GEXCON (2014) as part of the Buncefield Phase II project involved the modelling of various experimental cases using FLACS. Generally the code gave reasonably reliable predictions for continuously accelerating explosions in an enclosed experimental tunnel with sparsely distributed obstacles. This geometry corresponds closely to the type of test used in tuning the model.

However when applied to long linear arrays the predictions were in qualitative disagreement with experimental findings: instead of accelerating rapidly and attaining a steady state (or running away) the model predicted a flame that continued to increase in speed very slowly – over a distance of 100m (Figure 2).

The problem illustrated in Figure 2 can probably be traced to a lack of validation in open linear explosions that would have exposed structural weaknesses in the model. The flow induced by progress of a flame through a congested linear array in the open is fundamentally different to that observed in a similar array in a closed tube. In the open, the effect of the approaching explosion front (pressure and induced velocity) is only felt when the distance to the front is very close. This is not the case in enclosed explosions: all venting is along the axis of the enclosure and there is significant movement throughout the period of propagation of the flame. Figure 3 schematically illustrates this difference between enclosed and open linear explosions. In an enclosed explosion gas moves over a distance almost equal to the total flame propagation distance. On this trajectory it encounters obstacles spread out over almost all of the flame path and the final turbulence intensity, when gas is overtaken by the flame, may depend in some way on obstacles in the whole of the enclosed space. In this way the total distance travelled by the flame becomes a relevant length scale and this may explain the prediction of flame acceleration over very long distances. In the open the gas only moves by a distance comparable to the width of the array. There is no length scale in the problem of the order of 100m and the gradual, sustained increase in flame speed shown in Figure 2 is not expected.

CFD predictions of the sort illustrated in Figure 2 would be misleading and unhelpful in the assessment of the risk from rows of parked trailers because they suggest that the length of very long rows could be an important parameter in determining risk. The implication of the CFD result might be, for example, that a row of trailers 20-50 m long was acceptable but longer rows linked to higher flame speeds and pressures would not. This suggests potential controls and mitigation measures that, in fact, would not be effective.

Some CFD explosion codes have other deficiencies that make them unsuitable for linear explosions. For example, the thickness of the flame reaction zone relative to the array width is crucial in determining whether an explosion will run away or not. The reaction zone is a volume in which there are pockets of both burned and unburned gas. The expansion associated with combustion is spread out over this volume. If the width of the reaction zone is significant compared with the array width (or height) then expansion can be accommodated by sideways movement of gas. The speed of forwards flow of unburned gas past obstacles is then reduced and the explosion is weakened. This effect is illustrated in Figure 4. In the Buncefield Phase II tests reaction zone thicknesses were of order 1m: reduction of array width from 2m to 1m reduced the flame speed by almost a factor of two.

FLACS does not calculate the reaction zone thickness on physical grounds; instead the flame thickness is set for numerical convenience (GEXCON 2014). This means that the code does not allow for the weakening of explosion by side-venting in a meaningful, physically based way. Again, the effects of this deficiency would not be apparent in validation in enclosed or spherical geometries because side-venting is not possible in these cases.

Overall, whilst proprietary CFD explosion codes qualitatively show the effect of flame acceleration, they are not suitable for the detailed assessment of risks in the parked trailer problem.

HSL Method of analysis

The analysis is an extension of the method described by Atkinson 2012 and is largely based on measurements of turbulent burning velocity made by Gardner et al 1998. This experimental study is particularly suitable for the current problem because it involved flames propagating through arrays of obstacles that are a similar size to congestion elements under trailers and to the tree branches used in the Buncefield Phase II tests. The measured effective turbulent burning velocities

also extend to the range 40-60 m/s, which is the crucial range for dense arrays with the potential for flame runaway. It is worth noting that these effective velocities are much higher than the turbulent burning velocities reported in experiments with fan stirred bomb tests (Abdel-Gayed et al 1987) because of the folding of the flame around obstacles. Using Gardner et al's data directly avoids having to make assumptions about the effect of flame folding on burning rates. The data also clearly shows the effect of flame quenching at high obstacle densities (average turbulence intensities) and additional assumptions to account for this effect are not required.

Burning rate: The turbulent burning rate S_T is calculated in the new HSL model as

$$S_T = k.\left(\frac{S_L}{S_L^{ref}}\right).u'^{0.2}$$ with the constant k = 29.5 (SI units)

The dependence of S_T on u' matches the recommendation of Gardner et al for high Karlowitz Numbers. The coefficient k used in the model is also in line with Gardner et al's data.

Gardner et al did not explore how burning rates varied with the S_L – the laminar burning velocity of the gas mixture. The dependence of S_T on S_L is taken from Gülder 1990 $S_T \propto S_L^{0.75}$. The exponent is also close to the value recommended by Bray 1990 $S_T \propto S_L^{0.784}$. Laminar burning velocities S_L and the pressure sensitivity of S_L for stoichiometric propane and methane are shown in the table below (Poinsot and Veynante 2005). Propane has a marginally higher burning velocity than methane at ambient pressure but this velocity rises much more rapidly for propane than for methane if the mixture is compressed.

	S_L^0(at ambient pressure)	S_L after adiabatic compression
Methane	0.37 m/s	$(P/P_0)^{0.086}$ S_L^0
Propane	0.42 m/s	$(P/P_0)^{0.463}$ S_L^0

In this paper the model is applied to obstacles of a roughly similar size to those in the experiments on which the burning rate estimates are based, so the issue of scale is not pressing. Most authors agree that the dependence of burning rate on turbulent scale is relatively weak – for example Bray suggests $S_T \propto D^{0.196}$ where D is the turbulent length scale. This issue would have to be revisited if the model were applied to flames accelerating in arrays of much larger obstacles.

Induced flow : The model uses the following equation for forward velocity of unburned gas driven by the flame.

$$V_u = \left[\left(\frac{P_{\max}}{P_0}\right)^{\frac{1}{2\gamma}}.\sqrt{E} - 1\right].S_T$$

This expression closely matches experimental data and the results of CFD calculations for explosion pressures up to about 50kPa (Atkinson 2014). Other important relationships between P, E and S_T are

$$E = E_0\left(\frac{P_{\max}}{P_b}\right)^{\frac{1}{\gamma}}, \qquad P_{\max} - P_b = (E-1).\rho_u S_T^2$$

Thickness of reaction zone: The thickness of the reaction zone is assumed to be a function of the obstacle spacing and burning rate. For problems (TYPE A) that involve grids of obstacles that are relatively well separated in the stream wise direction the thickness of the reaction zone RZ is calculated as 2.5 times D_{obs} or G_{obs} whichever is greater. For problems (TYPE B) where obstacle spacings in the transverse and streamwise directions are similar (e.g. Buncefield Phase II arrays) the thickness of the reaction zone is taken as RZ = 0.7 / Area Blockage Density (ABD). In both cases the coefficients are chosen to match the observed thickness of the reaction zone in relevant experiments (Atkinson 2014).The thickness of the reaction zone is also assumed to be inversely proportional to the laminar burning rate. This does destabilise the flame a little but is a much less strong driver towards flame runway than the direct effect of flame speed on the maximum pressure of the unburned gas.

Side venting: For TYPE A problems forwards and side venting is generally unobstructed by obstacles and it is assumed that expansion through the forwards and sideways facing boundaries of the RZ is in proportion to their open areas. For TYPE B problems, venting from the RZ is obstructed and it is assumed that the flow through the various faces of the RZ is in proportion to the area of each face divided by the distance through the obstacle array that the flow must be forced. Flow resistance associated with obstacles is assumed to be isotropic.

Turbulent velocity: It is assumed that the turbulent intensity is a function of the Area Blockage ratio (ABR) in the most obstructed planes of the array (perpendicular to the direction of explosion propagation). For TYPE A problems this is the area blockage ratio in constituent grids. For TYPE B problems the ABR is calculated for an equivalent uniform grid of circular cylinders – i.e one which matches both the ABD and Volume Blockage Ratio (VBR) of the array. In both cases the relationship between u' and ABR is based on data in Gardner et al.

Method of solution: For a given geometry the model comprises a set of simultaneous equations for S_T, P_{max}, E, RZ and u'. These equations cannot be solved analytically but numerical solution is straightforward using an iterative method. An initial value of burning velocity (assuming low pressure) is used to determine initial values of other variables. These are then used to form a revised value of burning velocity and so on. Some typical results are shown in Figure 5. For values of VBR (obstacle density) under 3.4% the values of S_T, ΔP, E etc. converge. The solution corresponds to a steady sub-sonic flame. However, at value of 3.6% or higher no solution can be found. This corresponds to a set of circumstances in which a flame cannot propagate steadily but must continuously increase in speed or run away.

The current modelling casts no light on what eventually happens in cases where flames do run away: the flame speed will continue to rise beyond the range of validity of the equations used. Observations by British Gas, Baker Risk and GL suggest that final pressure in such cases is at least an order of magnitude greater than the fastest steady flames. Deflagration to detonation transition has regularly been observed if the array is long enough

Application of the modelling to the Buncefield JIP data

The results of recent Buncefield JIP Phase II WP3 tests provide an opportunity to evaluate analytical models of flame propagation. Seven experiments were carried out on congestion arrays formed from alder trees and one test with Norway spruce (SCI 2014). The constituent trees were typically 4-6m high and were cut to fit in a 3m high combustion rig. Upper parts of the trees were also fitted into the rig. The trunk butt size was around 75mm. A number of sample trees were broken down into elements of constant diameter and the quantity of branches in various size ranges determined. Overall values of VBR and ABD were determined. Similar (near stoichiometric) propane/air mixtures were used for all tests.

The main variables in the tests were:

i. Density of the congestion elements in the arrays (by varying the number of trees per square metre)

ii. Width of the array

The dissection analyses of tree structure did not cover leaves and associated fine stems. Photographs of the arrays were taken from the side of the rig but a consistent distinct background was not provided, so optical porosity can only be judged qualitatively. Area blockage density in Test 4 appears to have been dominated by leaves, so this test cannot be modelled.

Trees were reused for explosion tests – sometimes repeatedly. A significant proportion of area blockage in new trees is associated with small stems (<5mm in diameter). These are particularly vulnerable to being lost if the trees are exposed to an explosion and then left, exposed to the elements, for long periods. It has been assumed in Tests 6, 7 and 8 that all twigs with diameters <5mm were lost from any trees that had previously used – reducing the ABD to about 80% of the initially measured level. Reused trees in Test 8 had all gone through at least two previous tests and were then compressed into a smaller volume which would have displaced many elements larger than 5mm in diameter. It has been assumed in this case that the final ABD was around 70% of that for fresh trees.

Model results for conditions corresponding the JIP tests are summarised in Figure 6. The width of the array changed in Test 5 giving two different (steady) speeds. The analysis matches some of the most important features of the data set.

i. Rapid fall off in flame speed as the array width is reduced in comparison with the thickness of the reaction zone: - compare Test 5 (narrow) and Test 5 (wide).

ii. Moderate decreases in flame speed as smaller twigs are lost between repeat tests with the same array: - compare Test 6 and Test 7

iii. Onset of flame runaway at high obstacle densities: - compare Test 8 which gives a high steady flame in the model and in the experiment and Test 2 which is predicted to run away and was observed to lead to DDT.

Figure 7 shows model predictions for the final flame speed for a range of values of VBR for linear arrays of different cross-section. As expected wider and higher arrays produce higher flame speeds because the effects of side-venting are reduced. The final maximum flame speed and pressure before runaway are similar for both sizes of array. These flame speeds and pressures are close to the maximum values observed in the JIP tests. The model results provide some insight into the range of flame speeds (up to 150 m/s) that were observed in the tests and may be possible in other circumstances.

Application of the HSL model to explosions under rows of trailers

Figure 8 shows the results of the new HSL explosion analysis for stoichiometric propane and methane under a row of HGV trailers (with tractor units attached). In all of the results presented the "trailer spacing" is the total width of the slot occupied by the vehicle: spacings in the range 3 – 4 m were investigated. In all cases the width of the vehicles was assumed to be 2.55m so that the clearance between adjacent vehicles was 0.45m to 1.45m. A range of values of ABR have been examined. In all cases it is assumed that, in the plane of maximum ABR, congestion is provided by two objects that are regularly spaced in the vertical direction. In parts of the trailer where blockage is dominated by tyres and mudguards this is a somewhat conservative assumption. In other parts of the trailer there may be a variety of other guards, pipework, vessels etc.

The spacing between tankers for the calculations in Figure 8 is similar to that determined by investigators at the St Herblain incident (3.5 metres).

For propane the analysis indicates that steady flames are only possible for values of ABR < 0.3. If the space under the tanker is more congested than this, the flame will run away and a high order explosion of some sort will result. Since the flame speeds in the main constituents of gasoline vapour are similar to propane and vary in a similar way with pressure, these results are consistent with the observations at St Herblain and in other similar incidents.

For methane, explosion pressures are below 20 kPa (200 mbar) across the range of values of ABR. The pressure falls at high values of ABR because the forward flow through the obstacle array is increasingly obstructed and the reaction zone extends as the forwards flow takes the character of widely spaced jets. All calculations have assumed that the mixture is at ambient temperature. For LNG this is a somewhat conservative assumption.

Figure 9 compares cases where the trailers are attached to and detached from tractor units. Without the tractor the extent of venting of the space under the vehicle is marginally increased and higher values of ABR are required to produce a high order explosion. But overall venting is dominated by the gaps between trailers and so the effect of confinement provided by the tractor unit is not very large.

Figure 10 shows similar analyses for propane with a larger spacing (4m) between trailers. This spacing corresponds to the typical gap between trailer units as they are aligned with loading doors in a distribution centre. In this case no high order explosion is predicted if the tractor units are detached. Flame run away just occurs for a narrow range of ABR if the trailers are parked with tractor units. Explosion pressures for methane clouds are not shown but predictably are even lower than shown in Figure 10.

Figure 11 shows results for trailers parked very close together. High order explosions are predicted for propane for all but the lowest values of ABR. Even for such closely spaced trailers stoichiometric methane flames are not predicted to run away to cause a high order explosion. The main reason for this is the insensitivity of the laminar flame speed to adiabatic compression. In propane flames compression associated with the approaching flame leads to significant increases in burning rate which does not occur for methane.

Any scheme (e.g. GAMES) that predicts the reactivity of gases purely on the basis of the laminar flame speed may be misleading for linear arrays. The crucial question is: will the flame runaway and cause a high order explosion? In some circumstances the variation of burning velocity with adiabatic compression is more important in answering this question than the burning velocity at ambient pressure. This point is illustrated in Figure 12 that shows results for two fictitious gases. “Fake propane” has a flame speed that responds to pressure increases as propane but its flame speed at ambient pressure is that of methane. “Fake methane” has a flame speed that responds to pressure increases as methane but its flame speed at ambient pressure is that of propane. Only “Fake propane” gives a flame that runs away to a high order explosion.

It is worth noting that British Gas (Harris and Wickens 1989) demonstrated that methane can fuel a high order explosion in closely confined and congested conditions (e.g. a bang-box) and that once established a high order explosion (flame speed ~500m/s) can propagate without decay through congested arrays that are less strongly confined. This type of high speed flame spread is out of the range of the current analysis. DDT has not been observed in high order methane explosions in the open.

Application in risk assessment at a LNG site

The following example is based on a recent planning application for storage of liquefied natural gas (LNG). The LNG is to be used as a road fuel by a large logistics operator. Only limited details of the installation are available at the time of the assessment. 20 tonnes of LNG are to be stored in a small vacuum insulated vessel. Constraints on space have led to the vessel being located immediately adjacent to trailer parking areas with a total of 326 trailer parking spaces. Therefore a cautious best estimate assessment has been carried out in order to establish whether the hazards from a VCE arising from congestion formed by long linear arrays of parked trailers are significant when compared to other major accident events.

In addition to other major accident events such as jet fires are fireballs, there is the possibility of loss of containment events leading to the generation of a dense cloud of natural gas. If not ignited immediately by the events leading to the loss of containment, this could result in the spread of flammable vapour engulfing the arrays of parked trailers. A schematic of the layout is shown in Figure 13. There are three separate trailer parking locations. Trailers are parked in 2 rows in each area.

Information provided with the application indicates that trailer parking spaces are 3.5m wide, trailers are 2.5 m wide and the separation between adjacent trailers is 1m. The size of trailers and an estimate of the space under each trailer have been based on information provided by the applicant. As the space between the rows of trailers is less than twice the depth of the array, a trailer length, it has been assumed that the flame front will propagate between the rows; and in the same way around the array (van den Berg and Mos 2005).

The following congested volumes have been estimated:

- Area 1 - 73 parked trailers. Volume under each trailer (13.6 m x 2.5 m x 1.7 m) = 58 m3; volume in between each trailer (1.0 m x 4.2 m x 13.6 m) = 57 m3. Total congested volume for Area 1 = (73 x 58 + 71 x 57) = 8281 m3
- Area 2 - 124 parked trailers. Total congested volume for Area 2 = (124 x 58 + 122 x 57) = 14146 m3
- Area 3 - 129 parked trailers. Total congested volume for Area 3 = (129 x 58 + 127 x 57) = 14721 m3
- Total confined space for all three areas = 8281 + 14146 + 14721 = 37148 m3

As a cautious assessment it is assumed that the congested/confined volumes under and between the trailers parked in all three areas could be filled with a stoichiometric mixture of natural gas and air. The separation between these parking areas is not controlled in any way, therefore it is further assumed that an ignition of the gas cloud could propagate through the entire congested volume of 37148 m3.

Taking account of the consideration of methane in long linear array of parked trailers presented above, see in particular Figure 8 which relates to a similar type of array of vehicles, then it is judged that ignition of methane will not lead to sufficient flame acceleration to lead to a high order explosion. Therefore the overpressure from the VCE event has been estimated using the multi energy method, strength line 4 (Mercx et al 1998). This results in an estimated hazard range to 70 mbar, which HSE uses as the harm criterion for a sensitive population, of 106m. This hazard range is measured from the boundary of each parking area.

In conclusion the hazards from a VCE associated with long linear arrays of parked trailers are not significant when compared to the other major accident hazards for this installation.

Conclusions

1. Steady subsonic explosions in propane are possible in linear arrays up to a flame speed of around 150 m/s. Beyond this "runaway" to a high order explosion is likely. High order explosions hugely increase the risk because pressures are higher and more importantly there is a risk that the explosion may propagate into the whole of the rest of the cloud (including uncongested areas).
2. The main driver towards flame runaway is the increase in burning rate associated with adiabatic compression. Fuels for which such an increase is weak (e.g. methane) are unlikely to run up to high order explosions.
3. Some current CFD models perform badly when applied to linear explosions. More experimental work on linear explosions in the open is required to guide and validate development of codes.
4. Closely parked HGV trailers can provide the means to accelerate propane (and petrol vapour) explosions to high order. Maintaining a minimum parking slot widths of 4m greatly reduces the risk.
5. In the absence of strongly confined (bang box) ignitions directed under lines of trailers, it is very unlikely that explosions at small LNG sites will accelerate to give high order explosions.

Disclaimer

This publication and the work it describes were funded by the Health and Safety Executive (HSE). Its contents, including any opinions and/or conclusions expressed, are those of the authors alone and do not necessarily reflect HSE policy.

References

Abdel-Gayed, R.G., Bradley, D. and Lawes, M. (1987) *Turbulent burning velocities: A general correlation in terms of straining rates,* Proc. R. Soc. Lond. A 414.

Atkinson, G. (2012) *Effects of constraints on gas flow on the severity of vapour cloud explosions*, IChemE Symposium 158.

Atkinson, G. (2014) *Assessment of explosion severity at small scale LNG sites,* HSL Report MH/14/66

Bradley, D., Lau, A.K.C. and Lawes, M. (1992), *Flame stretch rate as a determinant of turbulent burning velocity*, Phil. Trans. R. Soc. London A. (1992) , Vol 338, pp. 359-387.

Bray K.N.C. (1990). *Studies of the turbulent burning velocity*, Proc. R. Soc. Lond. A, 431, 315–335.

Gardner, C.L., Phylaktou, H. and Andrews, G.E. (1998) *Turbulent Reynolds number and turbulent flame quenching influences on explosion severity with implications for explosion scaling*, IChemE Symposium Series No. 144. pp. 279–292, Paper 23.

GEXCON (2014), *Final report Modelling the experiments of the Buncefield Project, Phase 2, WP3*, Report GexCon-2014-F46365-RA-1

Gülder, O. M. (1990) *Turbulent premixed flame propagation models for different combustion regimes* Twenty third Symposium (International) on Combustion, p. 743, The Combustion Institute.

Harris, R.J. and Wickens, M.J. (1989) *Understanding vapour cloud explosions – an experimental study*. 55th Autumn Meeting of the Institution of Gas Engineers, Kensington, U.K.

Lechaudel, J.F. and Mouilleau, Y. (1995) *Assessment of an accidental vapour cloud explosion,* Journal of Loss Prevention in the Process Industries, Vol , p377-388.

Mercx, W.P.M., van den Berg, A.C., van Leeuwen, D. (1998) *Application of correlations to quantify the source strength of vapour cloud explosions in realistic situations: Final report for the project: 'GAMES'* TNO Report 1998-C53.

Pierorazio, A.J., Thomas J.K., Baker, Q.A. and Ketchum D.E. (2005) *An update to the Baker-Strehlow-Tang Vapor Cloud Explosion Prediction Methodology Flame Speed Table*. Process Safety Progress, Vol 24, No. 1.

Poinsot, T. and Veynante, D. (2005) *Theoretical and Numerical Combustion*, Pub.R.T. Edwards Inc.

SCI (2014) *Dispersion and Explosion Characteristics of Large Vapour Clouds Volume 1 – Summary Report*, Steel Construction Institute, SCI Document ED023

van den Berg, A.C., Mos, A.L., (2005) Research to improve guidance on separation distance for the multi-energy method (RIGOS) HSE Research Report 369

List of symbols

ABR	Area blockage ratio for a 2D grid of obstacles (dimensionless)
ABD	Area blockage density for a 3D array of obstacles (m^2/m^3)
D	Turbulent length scale (m)
D_{obs}	Diameter of obstacles (m)
E	Flame expansion ratio (variable when unburned gas pressurised)
E_o	Flame expansion ratio (low pressure limit)
G_{obs}	Clearance (gap) between obstacles in an array (m)
Ka	Karlowitz number
P_{max}	Maximum pressure (in the unburned gas) (Pa)
P_b	Pressure in the burned gas behind the flame (Pa)
P_o	Ambient pressure (Pa)
RZ	Thickness of reaction zone (m)
S_T	Turbulent burning velocity (m/s)
S_L	Laminar burning velocity (m/s)
S_L^{ref}	Reference laminar burning velocity (0.42 m/s)
u’	Turbulence velocity (m/s)
V_u	Speed of unburned gas ahead of flame - relative to obstacles (m/s)
VBR	Volume Blockage Ratio for a 3D array (dimensionless)
γ	Specific heat ratio
υ	Kinematic viscosity (m^2/s)
ρ_u	Density of unburned gas (entering the flame)

Figure 1: Aerial view of a distribution centre showing lines of closely parked trailers

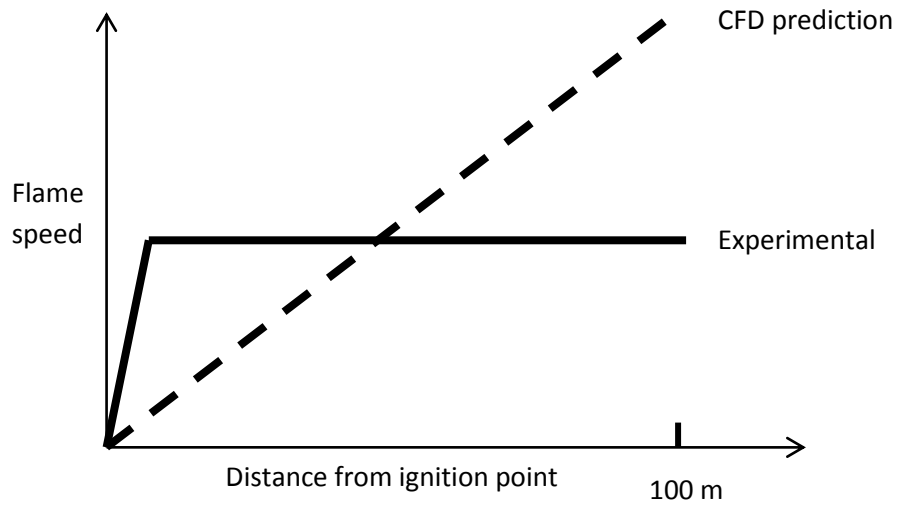

Figure 2: Schematic comparison of experimental finding and CFD prediction for flame acceleration a long linear array

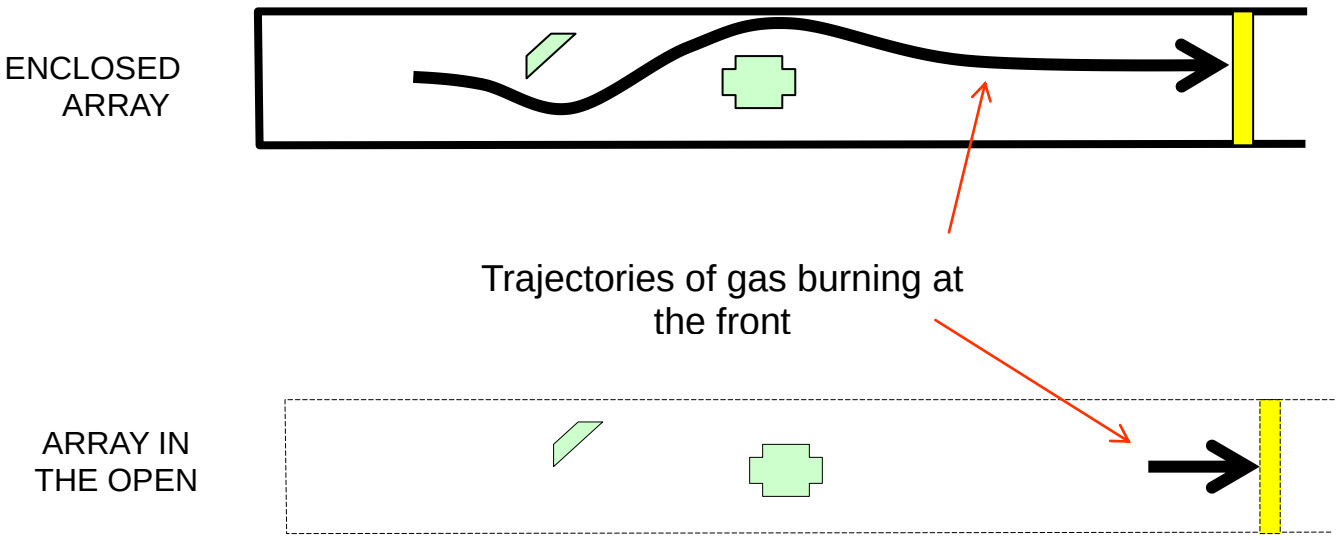

Figure 3: Schematic showing gas movement in enclosed and open linear explosions

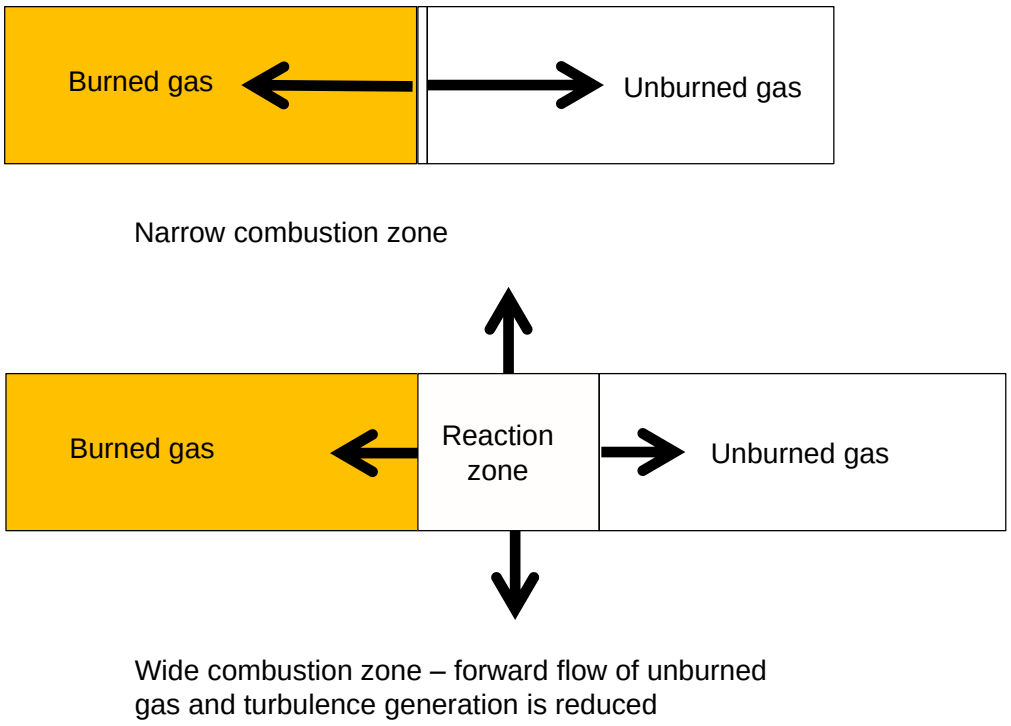

Figure 4: Effect of reaction zone thickness on venting of an explosion

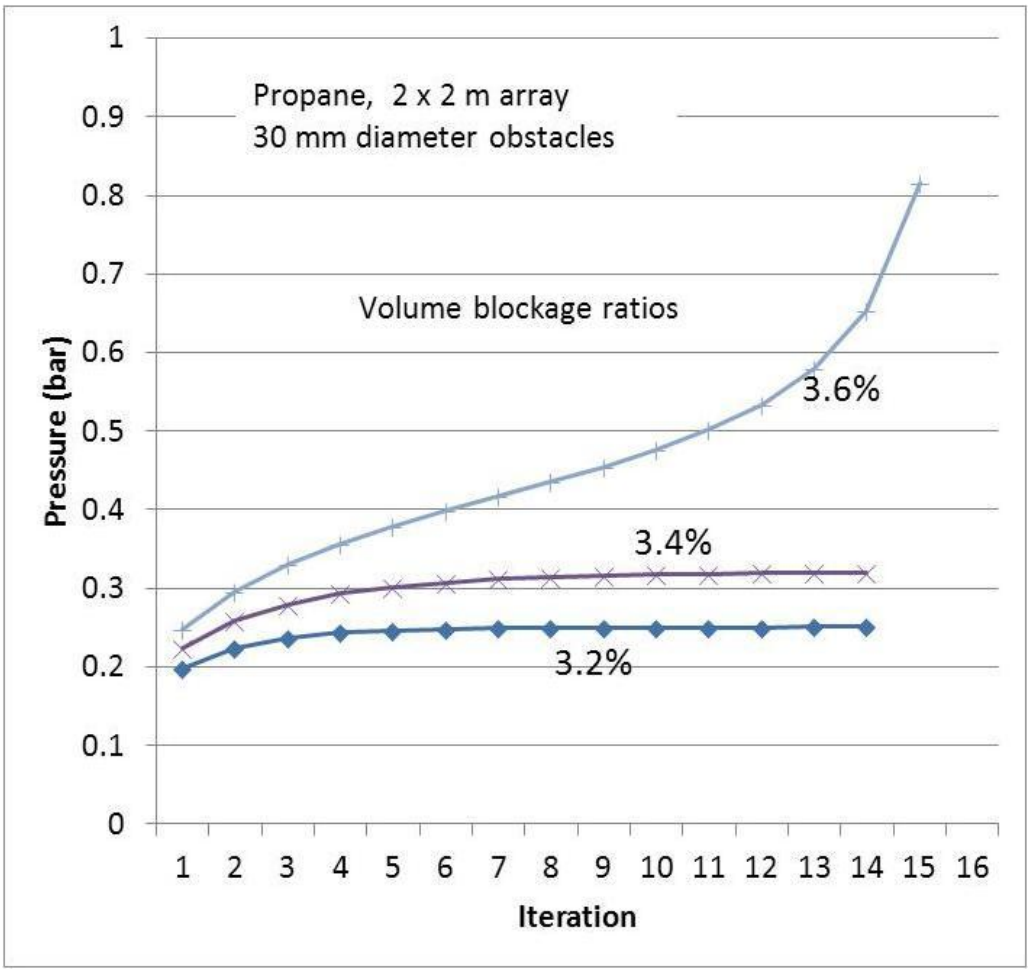

Figure 5: Model output for various values of volume blockage ratio (VBR).

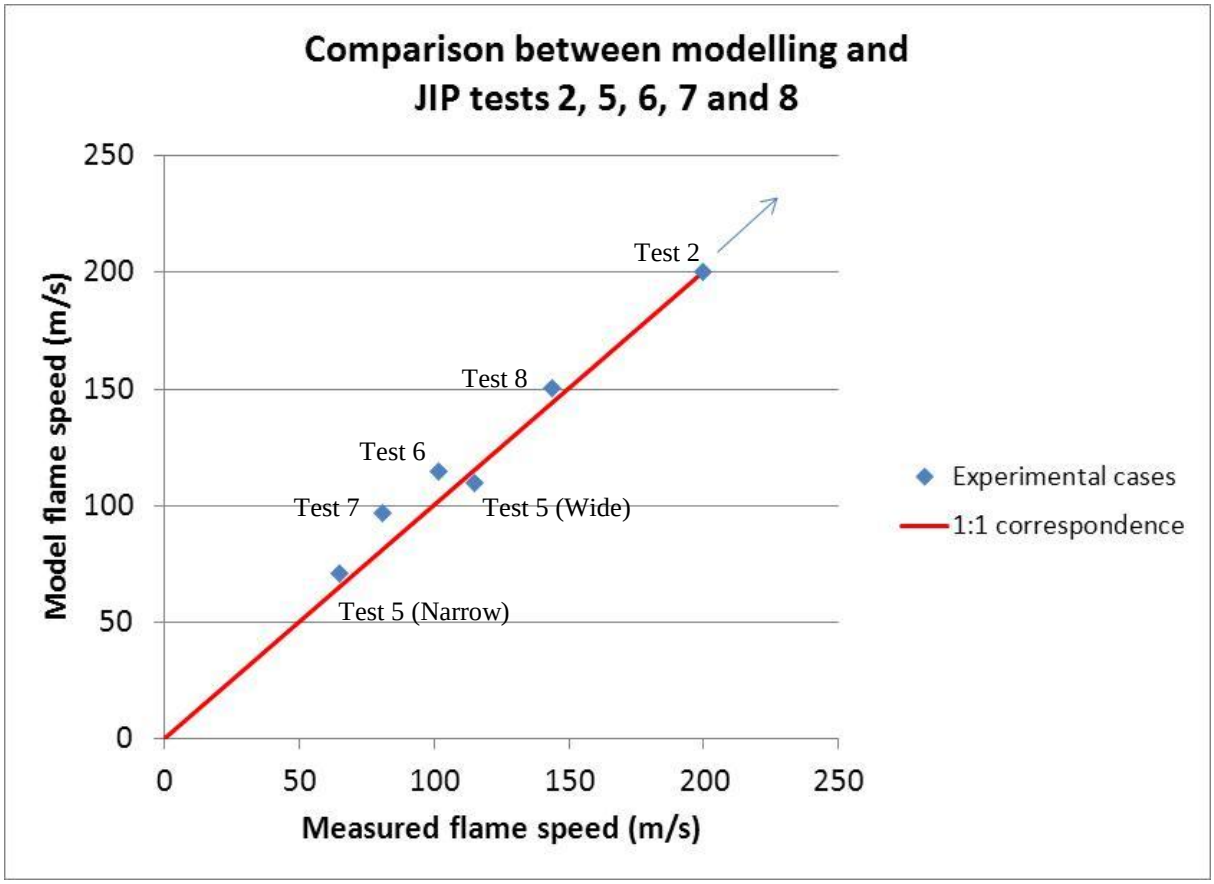

Figure 6: Comparison of measure and calculated flame propagation rates for steady flames observed in the Buncefield JIP tests. Note a measured speed of 200m/s indicates detonation and a calculated speed of 200 m/s indicates flame runaway in the model.

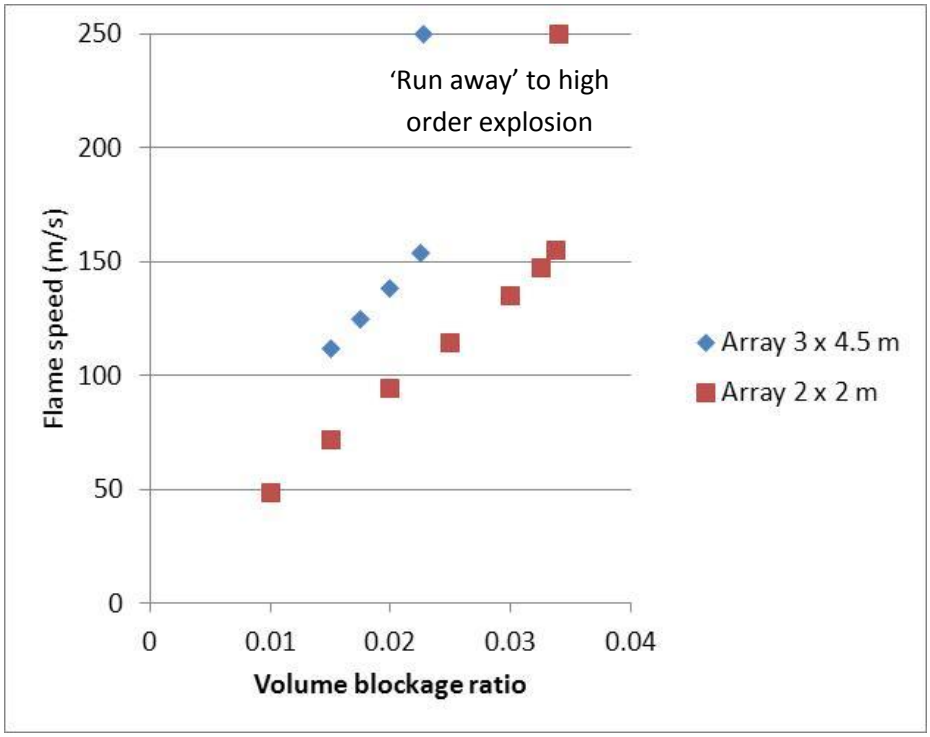

Figure 7: Flame speed variation with VBR - stoichiometric propane - obstacle size 30mm. The values of volume blockage ratio with flame speeds plotted as 250 m/s correspond to condition with no subsonic solution.

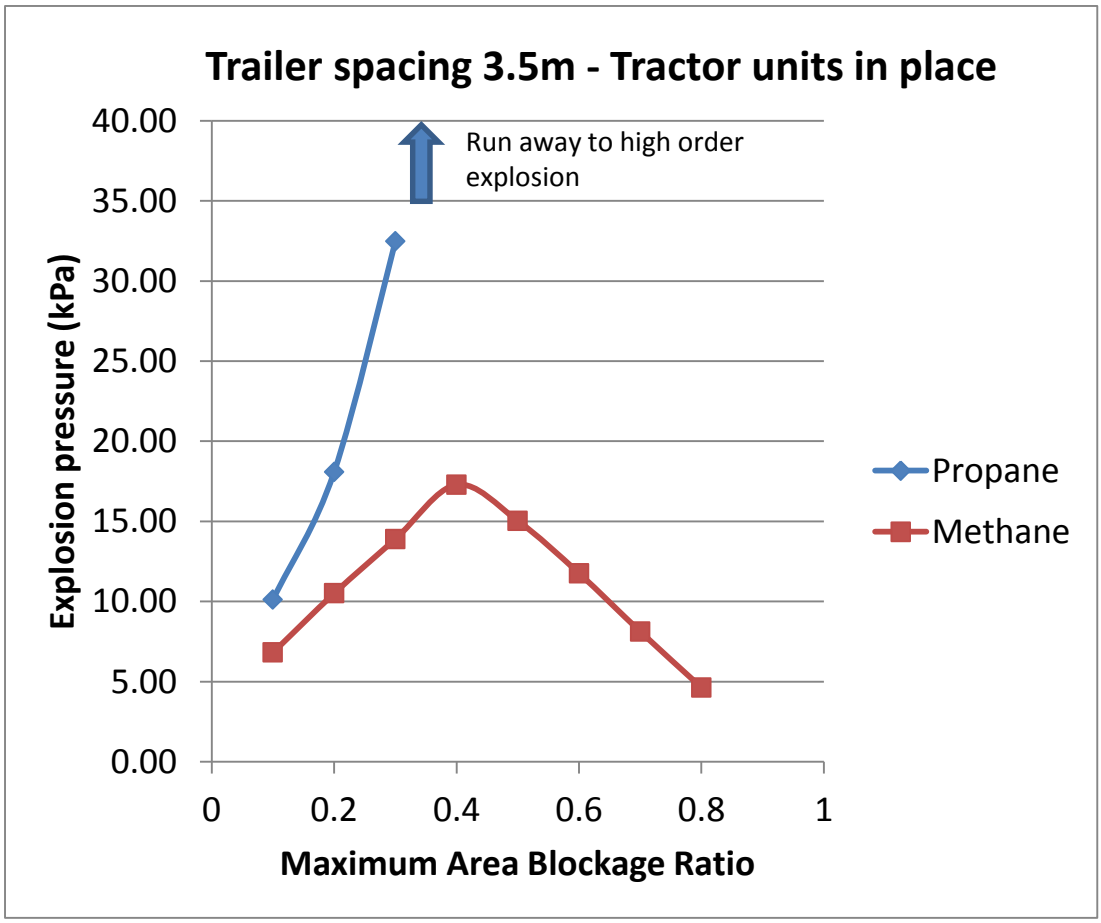

Figure 8: Explosion pressures for lines of trailers with tractors

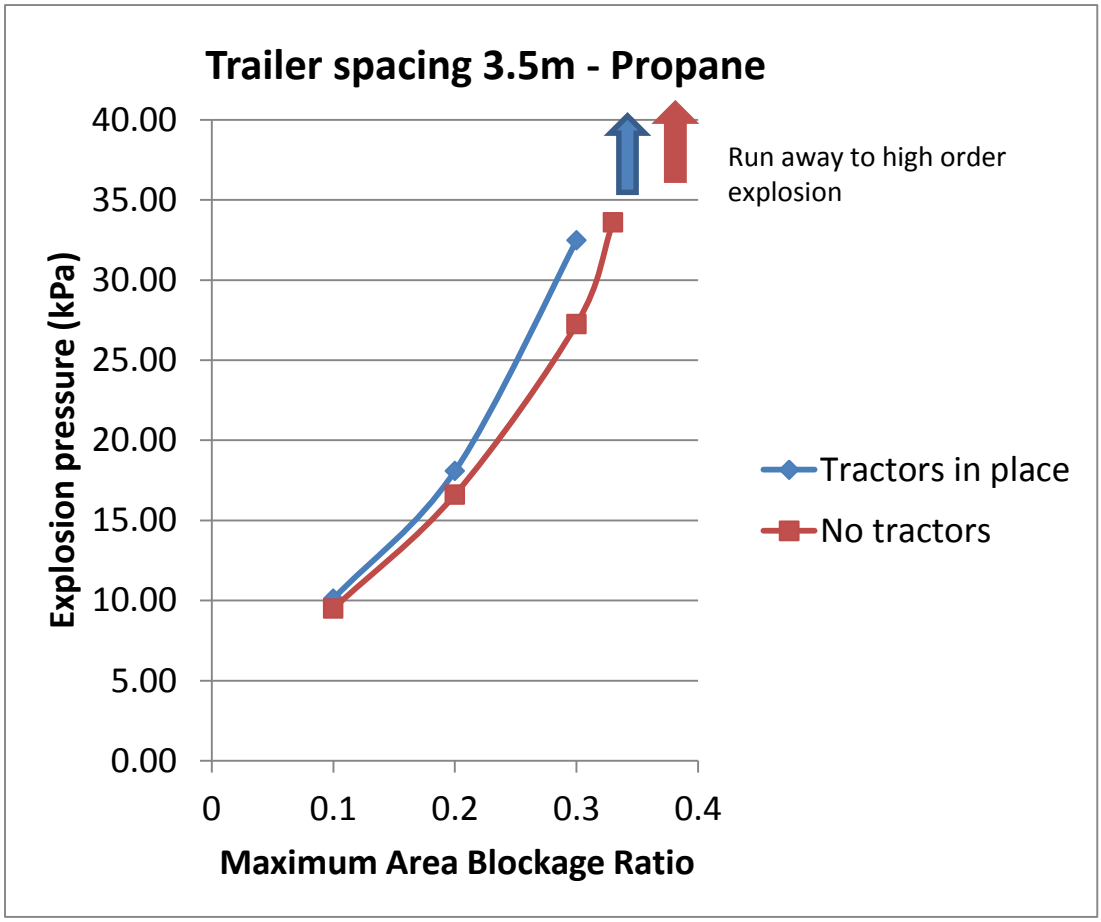

Figure 9: Explosion pressures with and without tractors units

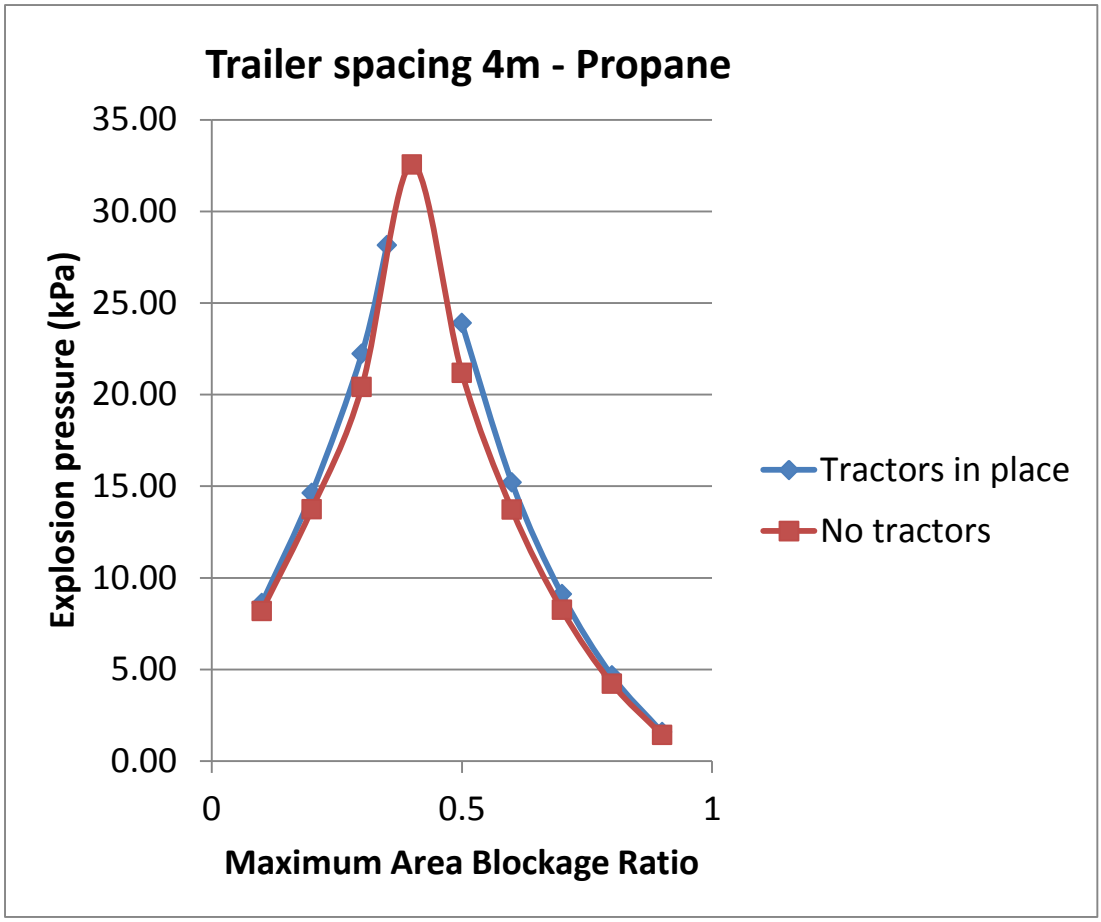

Figure 10: Explosion pressures for widely spaced trailers

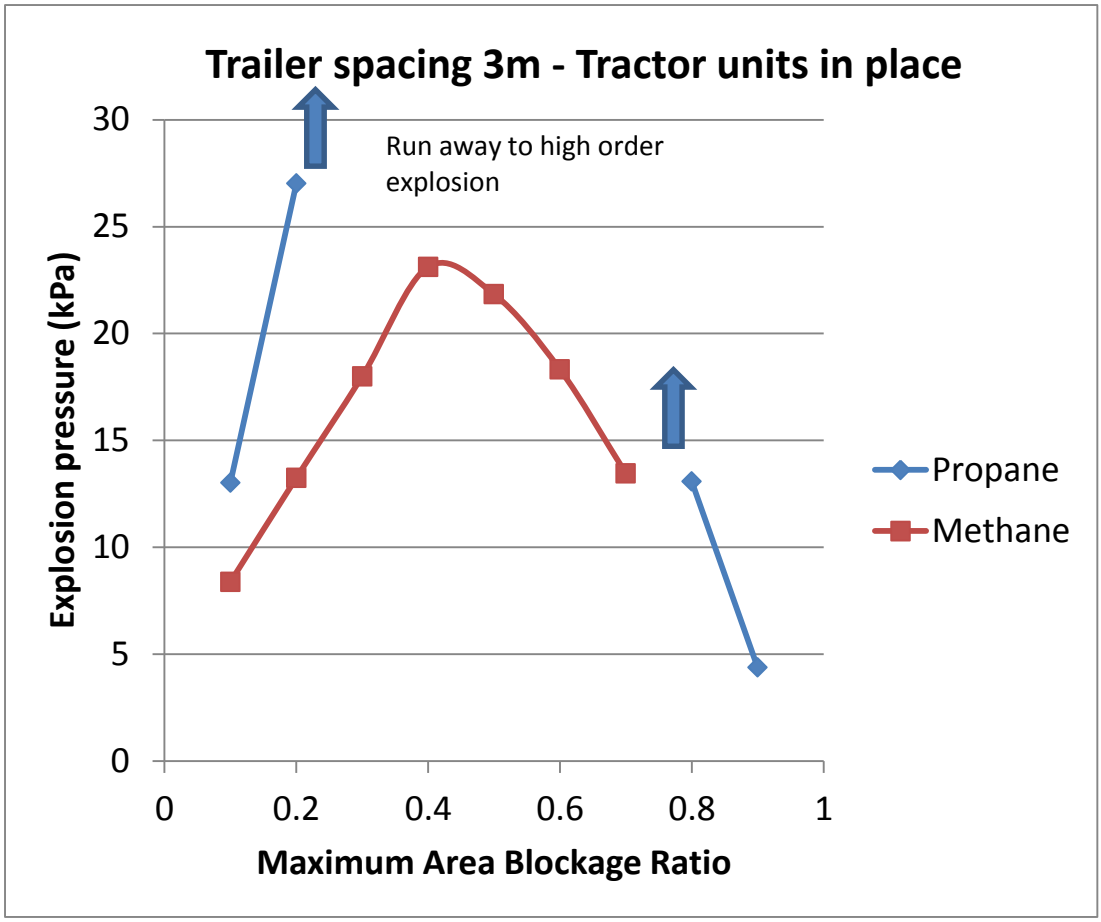

Figure 11: Explosion pressures for very closely spaced trailers

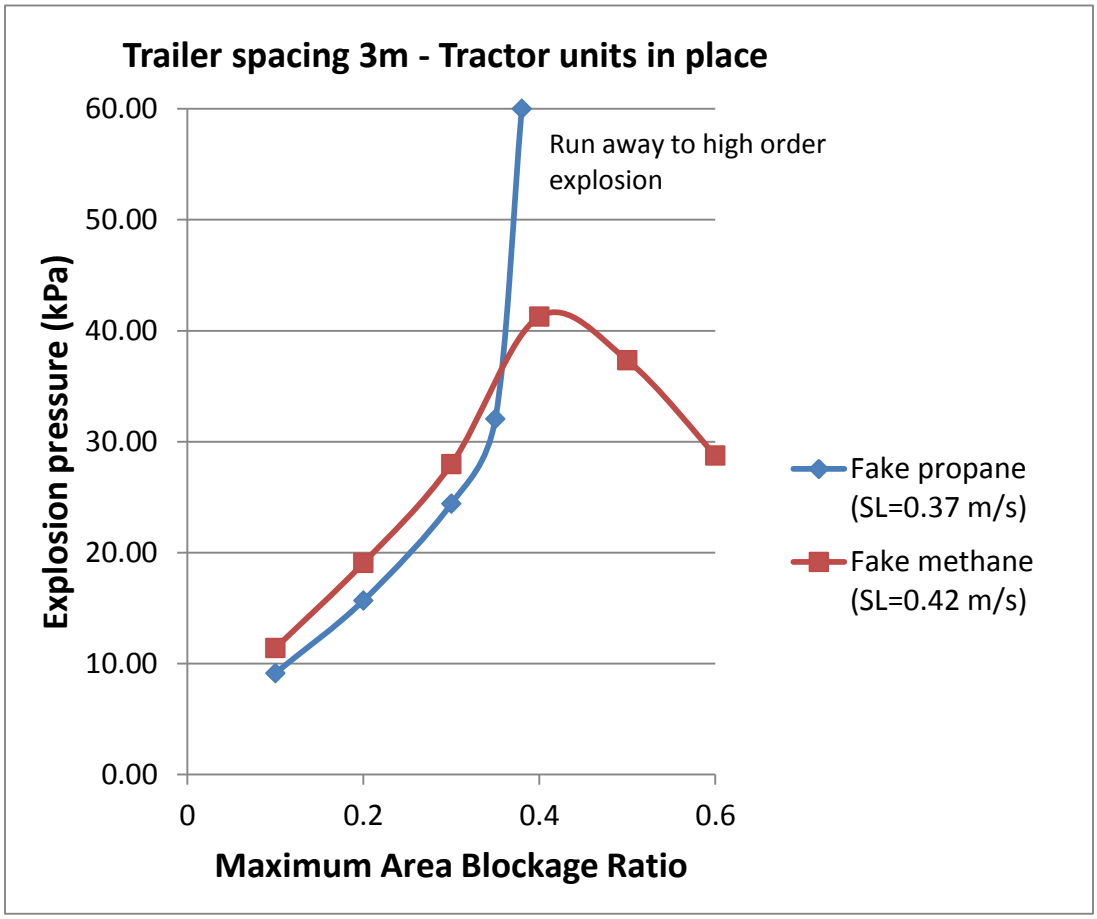

Figure 12: Illustration of the importance of pressure dependence of flame speed. Correct pressure dependence of laminar flame speed for propane and methane. Flame speeds at ambient pressure reversed.

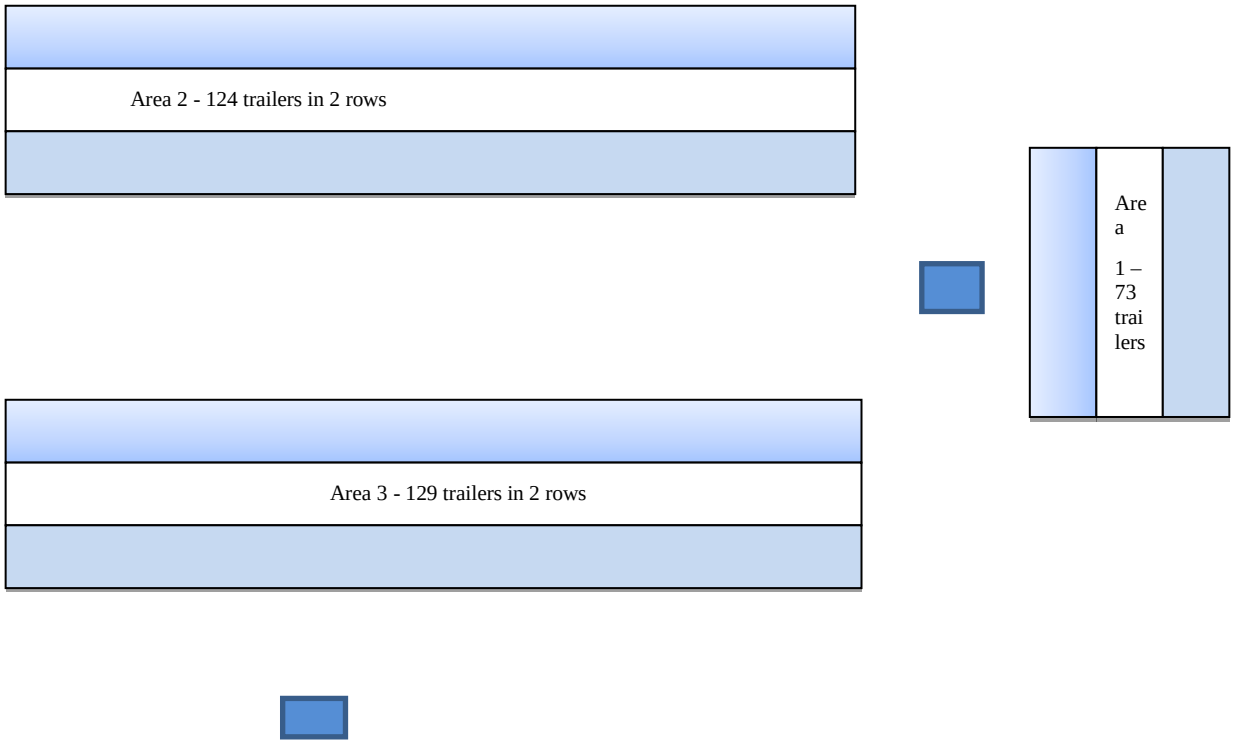

Figure 13: A schematic diagram of the layout of the LNG refuelling facility in relation to the trailer parking areas.